Zou et al. Cancer Nano (2021) 12:22
https://doi.org/10.1186/s12645-021-00093-9

Cancer Nanotechnology

RESEARCH Open Access

Emodin-loaded polymer-lipid hybrid nanoparticles enhance the sensitivity of breast cancer to doxorubicin by inhibiting epithelial–mesenchymal transition

Tengteng Zou[1†], Meng Lan[1†], Fengjie Liu[1†], Lihong Li[1], Tiange Cai[2*], Huaqin Tian[3*] and Yu Cai[1,4*]

*Correspondence: caitiange@163.com; 13929969262@139.com; caiyu8@sohu.com
†Tengteng Zou, Meng Lan and Fengjie Liu are co-first authors, and contributed equally to this work
[1] College of Pharmacy, Jinan University, Guangzhou 510632, People's Republic of China
[2] College of Life Sciences, Liaoning University, Shenyang 110036, People's Republic of China
[3] Foshan Hospital of Traditional Chinese Medicine, Foshan 528000, People's Republic of China
Full list of author information is available at the end of the article

Abstract

Background: The role of epithelial–mesenchymal transition (EMT) involved in breast cancer metastasis and chemoresistance has been increasingly recognized. However, it is necessary to search for more effective strategies to inhibit EMT thereby increase the sensitivity of breast cancer cells to chemotherapy drugs. Emodin has a potential in overcoming tumor drug resistance and restraining the development of EMT, but the poor internalization into breast cancer cells limited the application.

Results: MCF-7/ADR cells have more EMT characteristics than MCF-7 cell. EMT in MCF-7/ADR cells promotes the development of drug resistance via apoptosis resistance and facilitating the expression of P-gp. The anti-cancer effect of DOX enhanced by the decreasing of drug resistance protein P-gp and apoptosis-related proteins after EMT inhibited in MCF-7/ADR cells. E-PLNs increase the cellular uptake of EMO and restore DOX sensitivity in MCF-7/ADR cells by inhibiting EMT.

Conclusion: E-PLNs inhibit EMT to enhance the sensitivity of breast cancer to DOX. The combination of E-PLNs and DOX can improve the efficacy of DOX in the treatment of breast cancer, which provides a new method to prevent or delay clinical drug resistance.

Keywords: Emodin, Polymeric lipid nanoparticles, Breast cancer chemoresistance, Doxorubicin, Epithelial–mesenchymal transition

Background

Despite significant advances in cancer diagnosis and treatment, breast cancer to be the number one cancer in the world by 2020, more than 90% of the death causes of breast cancer patients are related to chemotherapy resistance (Siegel et al. 2021; Sung et al. 2021). The role of epithelial–mesenchymal transition (EMT) involved in chemotherapy resistance has been increasingly recognized. Asiedu MK and his colleagues found that EMT induced by TGF-β pathway in breast cancer cells decreased the sensitivity to doxorubicin (DOX) and paclitaxel (Asiedu et al. 2014). Reversal tumor drug resistance

through EMT inhibition is a new strategy and search for a safe and effective EMT inhibitor is necessary.

Emodin (EMO), the active component of *Rheum rhabarbarum*, is proved to have anti-tumor activity in breast cancer (Sun et al. 2015). In addition, EMO has a potential in overcoming tumor drug resistance and restraining the development of EMT (Liu et al. 2020a, b; Fu et al. 2012; Lu et al. 2016; Gu et al. 2019). It can effectively increase the accumulation of doxorubicin (DOX) by downregulating the expression of P-gp in lung adenocarcinoma and colorectal carcinoma cells (Iyer et al. 2018). It was found that the combination of DOX and EMO effectively inhibit the expression of snail, twist and slug, thereby inhibiting cell proliferation and promote cell apoptosis (Liu et al. 2020a, b). This combination results the suppression of cell migration and invasion. However, the poor internalization into the breast cancer cells limited the application of EMO. Hence, improving EMO internalization in breast cancer cells tend to be a reliable way to enhance the anti-cancer effect of DOX. Furthermore, it remains to be elucidated whether the drug resistance reversal effect of EMO is dependent on the inhibition of EMT.

Nanoparticles loaded with anti-cancer drugs become an ideal formulation for reversing chemoresistance (Li et al. 2016; Markman et al. 2013). The tumor targeting effect of nanoparticles is basely depended on the enhanced permeability and retention (EPR) in tumor microenvironment (TME), thus drug accumulation increased in TME (Kalyane et al. 2019). Polymeric lipid nanoparticles (PLNs), designed to combine the advantages of both liposomes and polymeric nanoparticles (Mukherjee et al. 2019; Date et al. 2007), can meet the structural and property differences of various anti-cancer drugs, as well as the combination therapy strategy, making them a promising drug carrier (Jain et al. 2020, Mukerjee et al. 2012).

Targeting EMT is becoming one of the new strategies for drug resistance reversal in various tumors. In this study, the relationship of EMT and drug resistance was discussed. Here, we provided evidence for E-PLNs to improve the therapeutic effect of DOX on breast cancer. Further, the evidence concerning drug resistance reversal mechanism of E-PLNs in suppressing EMT is provided.

Results

EMT is associated with DOX resistance in breast cancer cells

We compared the effect of DOX on the viability of MCF-7 cells and MCF-7/ADR cells. As Fig. 1A, DOX shown less toxicity to MCF-7/ADR cells (IC50 = 124.1 μM) than MCF-7 cells (IC50 = 5.35 μM). MCF-7/ADR cells were resistant to DOX with a resistance index of 23.2. EMT is characterized by loss of E-cadherin expression and upregulated Vimentin and N-cadherin (Fig. 1B, C). DOX significantly induced EMT and enhanced invasion in MCF-7/ADR cells. (Fig. 1D, E).

EMT inhibiting cell proliferation and invasion

TGF-beta signaling has been shown to play an important role in EMT. Galunisertib, a selective TGF-β receptor type I (TGF-βRI) kinase inhibitor to block TGF-β signaling reverse EMT, is applicated in this part to investigate the relationship of EMT and drug resistance. It can be seen from Fig. 2A that different concentrations of Galunisertib can

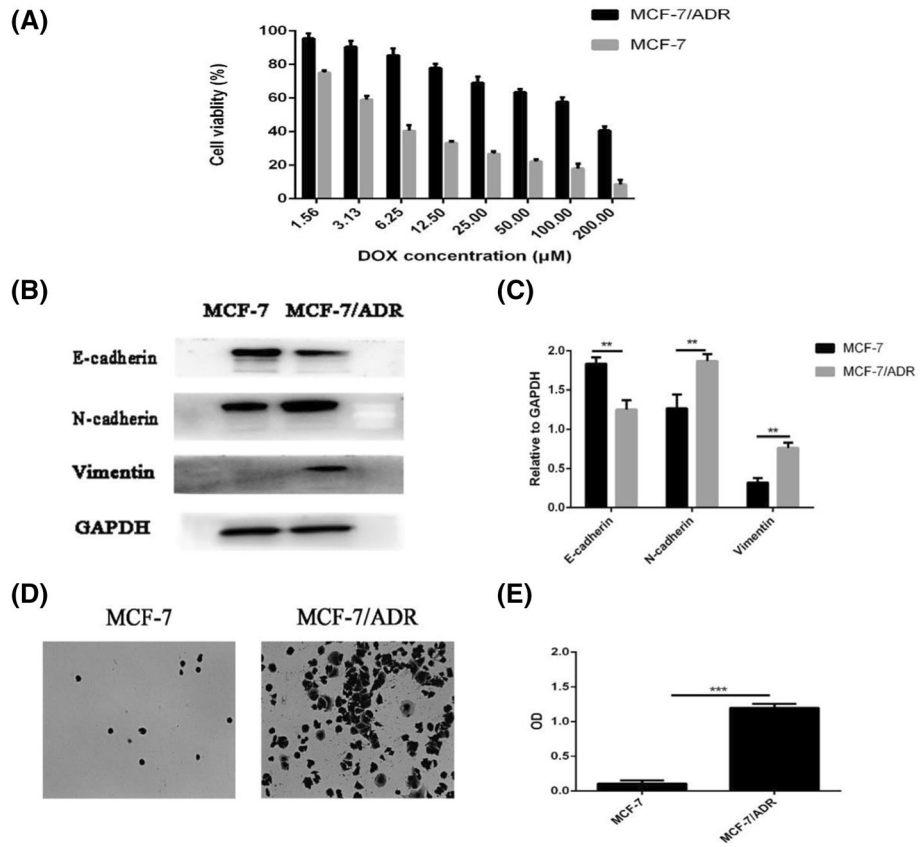

Fig. 1 EMT is associated with DOX resistance in breast cancer cells. **A** Cell viability in vitro on MCF-7 and MCF-7/ADR cells after treatment with different DOX concentration (1.56 μM-200 μM) for 48 h. **B**, **C** The expression of E-cadherin, N-cadherin and Vimentin in MCF-7 and MCF-7/ADR cells was analyzed by Western blotting. **D**, **E** The invasion activity of MCF-7 and MCF-7/ADR cells were observed and photographed with 200 × microscope, and the OD value was detected at 570 nm to indirectly reflect the number of cells. $N = 3$, $^{**}p < 0.01$, $^{***}p < 0.001$

inhibit the proliferation of MCF-7/ADR cells, and the IC50 value calculated is 248.2 μM. When the concentration of Galunisertib was 30 μM, the cell viability was more than 90%. Therefore, the concentration of 30 μM Galunisertib is selected to application for the subsequent experiment to exclude the interference of Galunisertib induced cytotoxicity. Galunisertib reversed EMT marker protein expression in the selected concentration (Fig. 2B, C). The therapeutic effect of DOX was improved under the incubation of 10 μM DOX and 30 μM Galunisertib (Fig. 2D) MCF-7/ADR cells have higher invasive ability than the DOX sensitive MCF-7 cells, but invasive ability of MCF-7/ADR cells treated with DOX did not change. Compared with DOX (10 μM) group, the invasion activity was decreased in Galunisertib (30 μM) group. DOX shows the enhanced cytotoxicity in MCF-7/ADR cells with the synergy of Galunisertib (Fig. 2E, F). These results suggest that the inhibition of EMT may weaken the drug resistance of MCF-7/ADR cells.

Blocking EMT restrains the expression of P-gp and induced apoptosis

Apoptosis is an important manifestation of anti-tumor effect of chemotherapy drugs. We can see from Fig. 3A, B that the apoptosis rate of DOX (10 μM) group is only

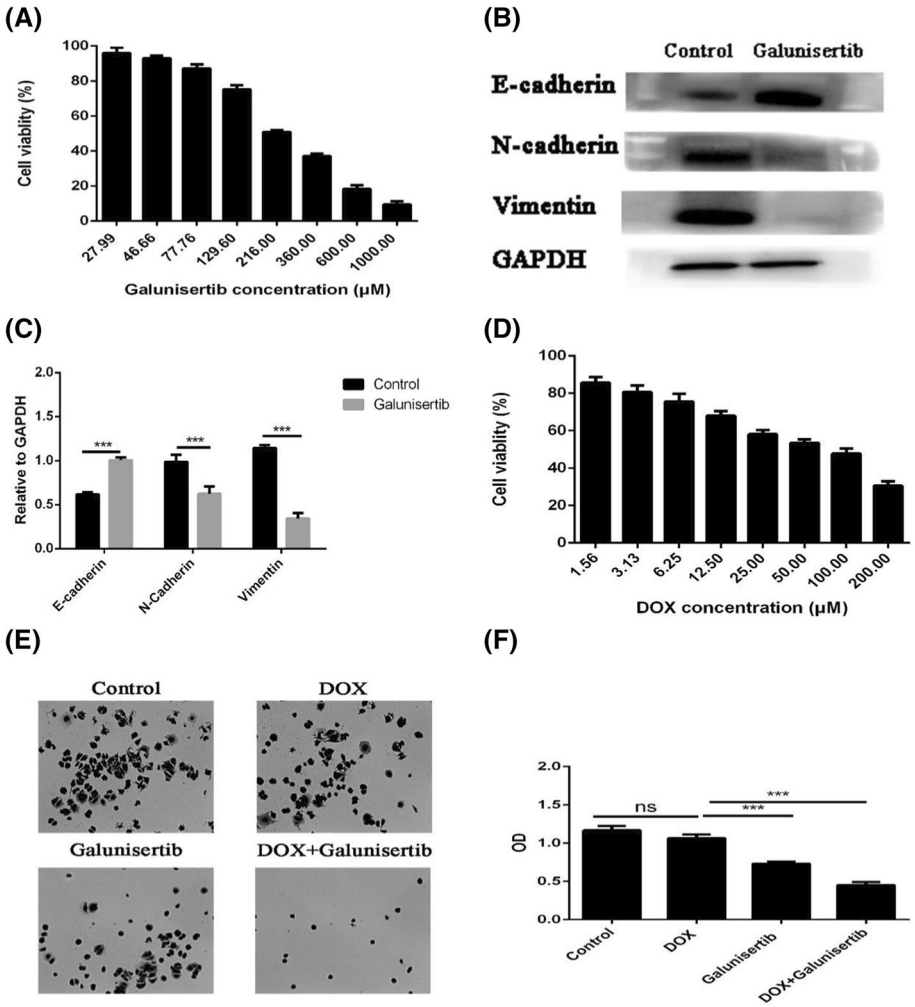

Fig. 2 The effect of Galunisertib combined with DOX on cell proliferation and invasion. Cell viability of MCF-7/ADR cells after treatment with different Galunisertib concentration (27.9–1000 μM). **B**, **C** The effect of 30 μM Galunisertib on the expression of EMT marker protein. $N = 3$, $^{**}p < 0.01$, $^{***}p < 0.001$ compared with Control group. **D** Cell viability on MCF-7/ADR cells after treatment with 30 μM Galunisertib combined with DOX of different concentrations (1.56–200 μM). **E**, **F** The invasion activity of MCF-7/ADR cells after incubation with DOX (10 μM), Galunisertib (30 μM), DOX (10 μM) + Galunisertib (30 μM) over 48 h. $N = 3$, $^{**}p < 0.01$, $^{***}p < 0.001$ compared with DOX group

13.81%, Galunisertib (30 μM) group (the apoptosis rate is 7.85%) has little effect on apoptosis. When DOX was combined with Galunisertib, the number of apoptotic cells increased, and the apoptotic rate was 23.88%. It can be seen from Fig. 3C, D that compared with DOX group, Bax/Bcl-2 ratio increased in DOX + Galunisertib (30 μM) group. These results suggest that inhibition of EMT can enhance DOX induced apoptosis in MCF-7/ADR cells.

EMT was closely related to the process of drug resistance, one of which was up-regulation of drug resistance related transporters. As can be seen in Fig. 3E, F, the difference of expression level of P-gp protein in Control group and DOX group was not significant. However, when MCF-7/ADR cells were treated with Galunisertib,

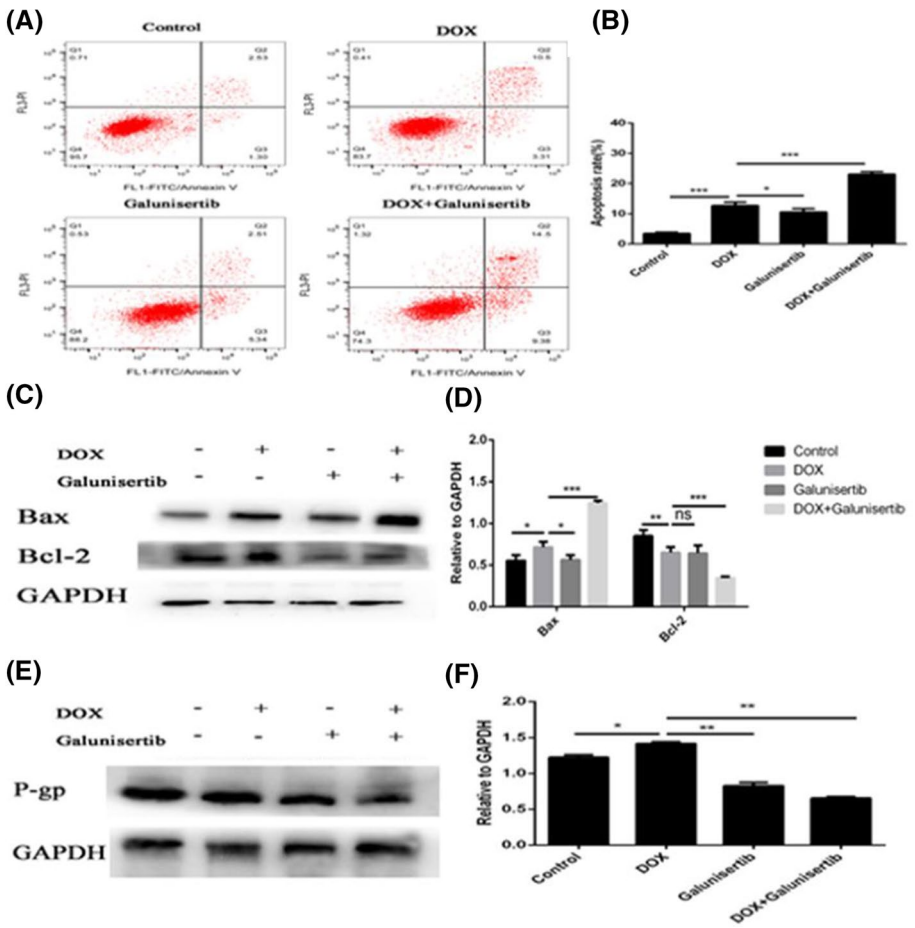

Fig. 3 Effect of Galunisertib combined with DOX on apoptosis and expression of drug resistance protein. **A**, **B** The apoptotic rate of MCF-7/ADR cells treated with different groups (DOX, Galunisertib, DOX + Galunisertib) was measured by flow cytometry. **C**, **D** The expression of Bax and Bcl-2 in MCF-7/ADR cells treated with DOX, Galunisertib, DOX + Galunisertib. Relative levels of the proteins were quantified by densitometric analysis. **E**, **F** The expression of P-gp and MRP1 in MCF-7/ADR cells treated with different groups (DOX, Galunisertib, DOX + Galunisertib). $N = 3$, $^{**}p < 0.01$, $^{***}p < 0.001$ compared with DOX group

the expression levels of P-gp protein were down-regulated. More importantly, the expression of P-gp in DOX + Galunisertib group was significantly suppressed than DOX group, resulting in decreasing of DOX efflux. Therefore, blocking EMT leads to down-regulated P-gp level, which restrains the DOX efflux in MCF-7/ADR cells.

E-PLNs increase the cellular uptake and cytotoxity of EMO

E-PLNs prepared by nano precipitation method as our group reported (Liu et al. 2021) are light yellow liquid (Fig. 4A). To preserve the samples for a long time, we keep E-PLNs samples through freeze-drying (Christ ALPHA 1–4 LD plus). The particle size of E-PLNs was 122.7 ± 1.03 nm (Fig. 4C), zeta potential was − 28.5 ± 1.55 mV (Fig. 4D) and PDI was 0.118. The results show that the nanoparticles have uniform size and good stability.

As E-PLNs have no fluorescence, the C-6 PLN, which loaded with 3-(2-benzothiazolyl)-*N*,*N*-diethylumbelliferylamine (coumarin-6,with green fluorescence), is formulated to

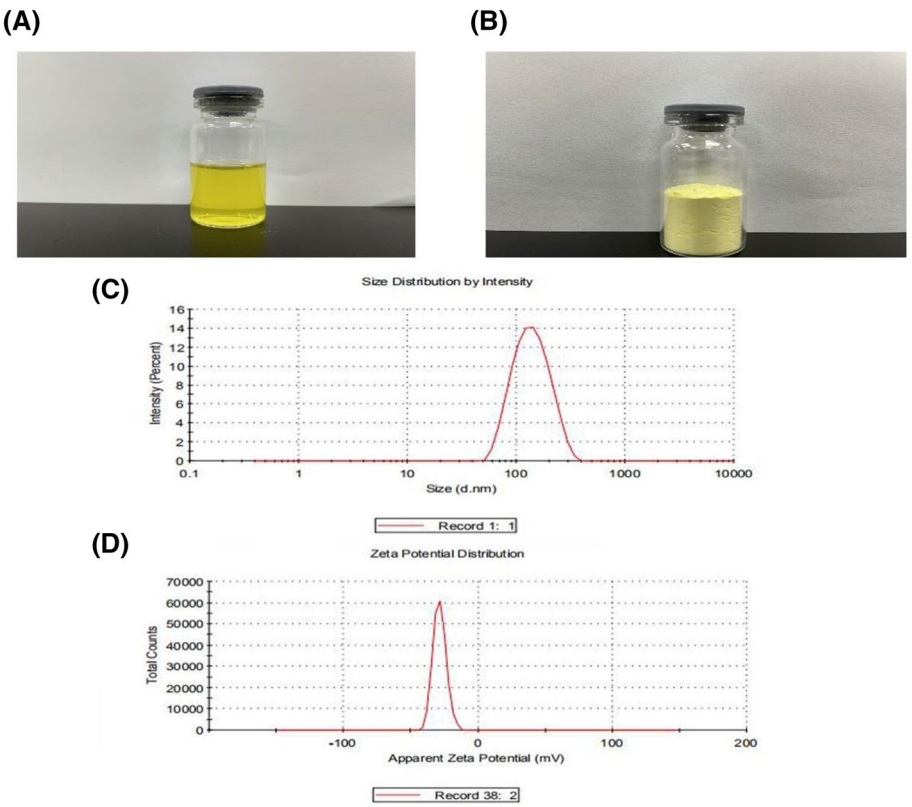

Fig. 4 The characterization of E-PLNs. **A** The morphology of E-PLNs. **B** Lyophilized powder of E-PLNs. **C**, **D** The particle size and Zeta potential of E-PLNs was measured by the laser particle size analyzer

analyze the cellular uptake of PLNs carriers. After the coumarin-6-labeled nanoparticles were internalized, the green fluorescence mainly distributed in the cytoplasm (Fig. 5A), indicating that PLNs carriers promote the cellular uptake of the loaded drugs. Furthermore, flow cytometry quantitatively analyzes cellular uptake, and the uptake intensity was expressed as the average fluorescence intensity of cells. The average fluorescence intensity of cells was 500, indicating that the cells had a high uptake of nanoparticles (Fig. 5B, C). The cytotoxicity of EMO group (Fig. 5D) and E-PLNs (Fig. 5E) group on MCF-7/ADR cells gradually increased with the increase of EMO concentration. The IC50 of EMO and E-PLNs were 150.5 μM and 138.7 μM, respectively. To further explore whether EMO or E-PLNs can enhance the toxicity of DOX, a suitable concentration was selected and combined with DOX to detect the effect on cell viability (Fig. 5F). We selected 30 μM EMO and E-PLNs for the subsequent combined administration experiment. It can be seen from Fig. 5F that 30 μM E-PLNs can enhance the cytotoxicity of different concentrations of DOX. Finally, 10 μM DOX was selected to explore how E-PLNs improve the therapeutic effect of DOX.

E-PLNs enhance the effect of DOX in apoptosis induction

MCF-7/ADR cells were treated with DOX, DOX + EMO, DOX + E-PLNs to investigate whether E-PLNs induced cell apoptosis. The morphological changes of apoptotic

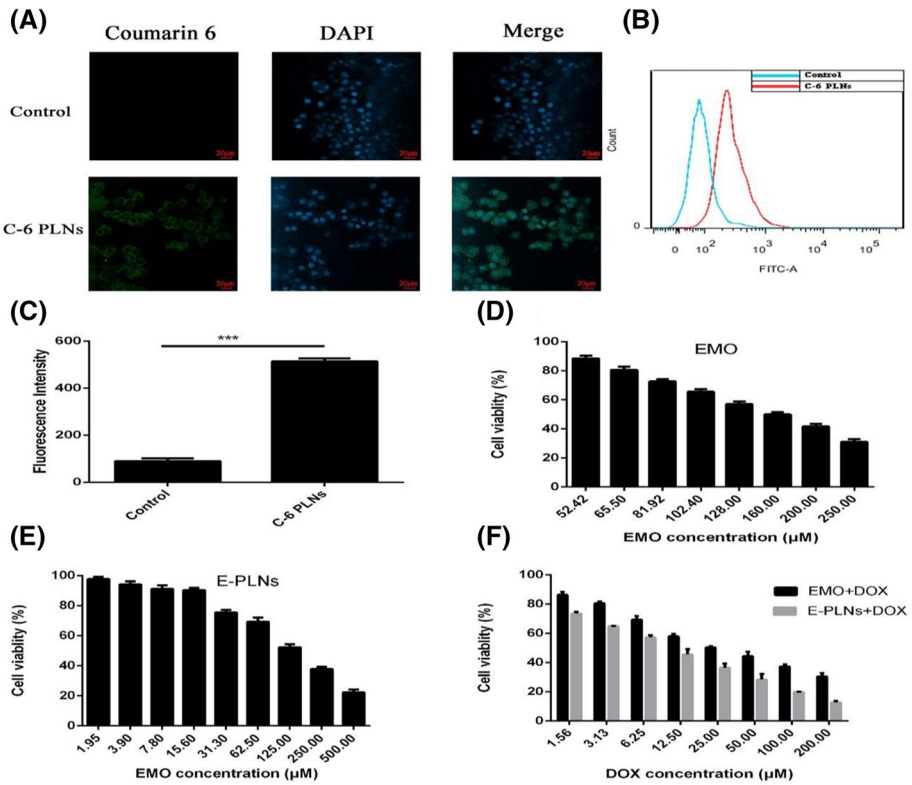

Fig. 5 Cellular uptake and cytotoxicity study of E-PLNs. **A** confocal imaging of C-6 PLNs in MCF-7/ADR cells was observed. **B**, **C** Flow cytometry and fluorescence intensity of nanoparticles uptake by MCF-7/ADR cells, $N = 3$, $^{**}p < 0.01$, $^{***}p < 0.001$ compared with Control group. **D**, **E** Cell viability in vitro on MCF-7/ADR cells after treatment with free EMO and E-PLNs. **F** The cell viability of MCF-7/ADR cells treated with 30 μM EMO or E-PLNs combined with different concentrations of DOX (1.56–200 μM)

cells are shown in Fig. 6A. We observed that the untreated cells were round or oval blue nuclei, while the cells in the treatment group were fragmented, and the number of apoptotic bodies was significantly improved in the E-PLNs group. It can be seen from Fig. 6B, C that compared with DOX (10 μM) group (15.52%), the apoptosis rates of DOX + EMO (30 μM) and DOX + E-PLNs (30 μM) groups were 18.49% and 24.48%, respectively, and the apoptosis rate was significantly increased by the synergy of DOX and E-PLNs. Western blot results also showed that the ratio of Bax/Bcl-2 was increased in DOX + EMO (30 μM) and DOX + E-PLNs (30 μM) groups, which indicated promoted cell apoptosis by DOX + E-PLNs. DOX + E-PLNs group showed a more significant effect on the expression of apoptotic protein (Fig. 6D, E). Flow cytometry combined with Western blot showed that E-PLNs may enhance the apoptosis inducing effect of DOX on MCF-7/ADR cells through affecting apoptosis-related proteins.

E-PLNs enhance DOX accumulation and restrain the expression of P-gp

The accumulation of DOX in MCF-7/ADR cells treated by different administration groups (Control, DOX, DOX + EMO, DOX + E-PLNs) was analyzed quantitatively by flow cytometry (Fig. 7A). From Fig. 7B, it can be seen that the peak map of DOX + EMO (30 μM) and DOX + E-PLNs (30 μM) groups shifts to the direction of high fluorescence

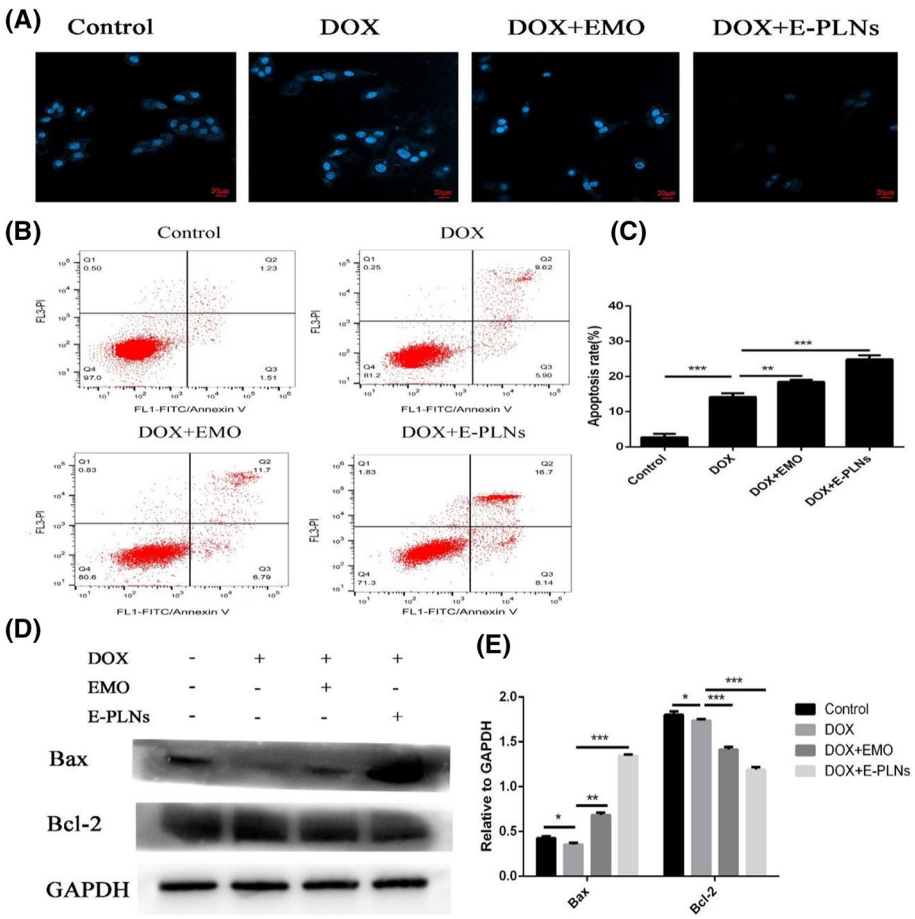

Fig. 6 E-PLNs enhanced DOX induced apoptosis by regulating apoptosis-related proteins. **A** Morphological changes of nuclei in MCF-7/ADR cells in the different treated groups using DAPI staining. **B**, **C** Apoptosis assay of MCF-7 cells after incubation with different treated groups. **D**, **E** The expression of Bax and Bcl-2 in MCF-7/ADR cells were determined by Western blot analysis. $N = 3$, $^{**}p < 0.01$, $^{***}p < 0.001$ compared with DOX group

intensity compared with DOX (10 μM) group. The average fluorescence intensity of DOX + E-PLNs is higher than that of DOX group, indicated that E-PLNs promote the uptake of DOX and increase the DOX accumulation in MCF-7/ADR cells. In addition, the expression of P-gp significantly decreased in DOX + EMO and DOX + E-PLNs groups compared with control and DOX groups (Fig. 7C, D), indicating that E-PLNs could effectively inhibit the expression of P-gp protein thus enhancing the effect of DOX.

E-PLNs inhibit the expression of EMT marker protein and cell invasion

The expression of E-cadherin decreased, while the expression of N-cadherin and Vimentin increased in MCF-7/ADR cells, which indicated the occurrence of EMT. It can be seen from Fig. 8A, B that there is no significant difference in the protein levels of E-cadherin between the Control group and the DOX group, but the protein level of N-cadherin increases significantly, which indicates that DOX administration to MCF-7/ADR cells may further promote EMT. In DOX + E-PLNs (30 μM) group, the expression of E-cadherin protein was increased, and the expression of vimentin and N-cadherin

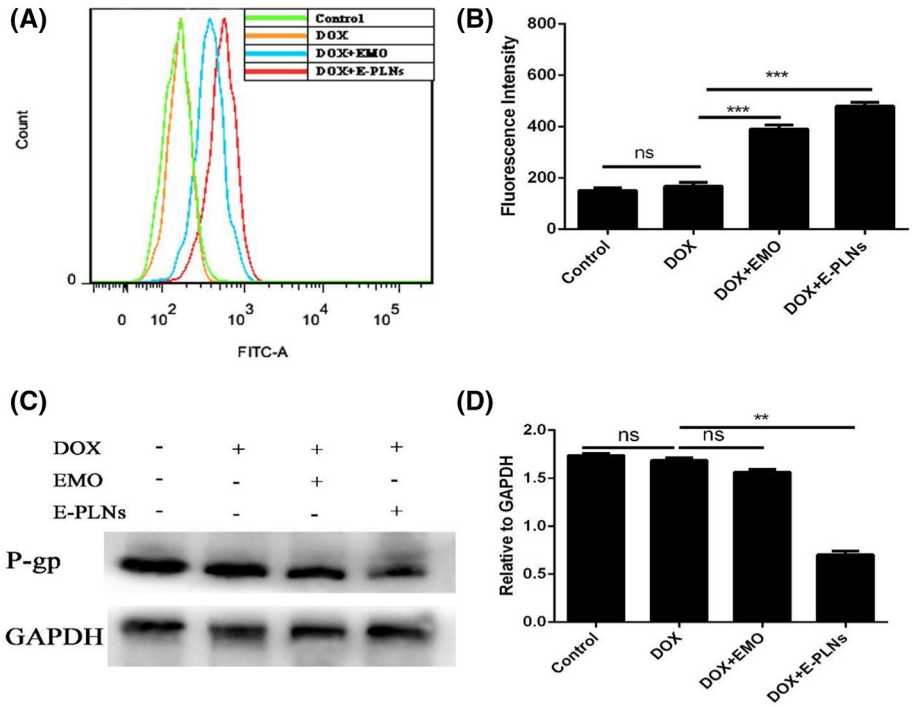

Fig. 7 E-PLNs increase the accumulation of DOX by inhibiting the expression of drug resistance protein. **A**, **B** The accumulation of in MCF-7/ADR cells treated with DOX, DOX + EMO, DOX + E-PLNs measured by flow cytometry. **C**, **D** The expression of P-gp in MCF-7/ADR cells detected by Western blotting analysis. $N = 3$, $^{**}p < 0.01$, $^{***}p < 0.001$ compared with DOX group

protein was down-regulated. These results indicate that E-PLNs can effectively inhibit EMT, and the enhancement of DOX sensitivity of MCF-7/ADR cells by E-PLNs is related to the inhibition of EMT.

Cell invasion is an important manifestation after EMT induction. In Fig. 8C, D, there was no significant difference in the number of cell invasion between the Control group and DOX group. Compared with DOX group, the number of invasive cells in DOX + EMO (30 μM) group and DOX + E-PLNs (30 μM) group decreased, and DOX + E-PLNs group was more significant. These results shown that the combination of E-PLNs and DOX can inhibit the occurrence of EMT and the tendency to invasion in MCF-7/ADR cells.

Discussion

Chemotherapy is the main treatment for early stage of breast cancer, but the sensitivity of tumor cells to chemotherapeutic drugs decreases with long-term chemotherapy. Increasing evidence shown that EMT is involved in the development of drug resistance in breast cancer (Jiang et al. 2017). After EMT was induced by snail eukaryotic expression vector, the expression of BCRP was significantly increased and the drug resistance of MCF-7 cells was increased to 9.93 times (Du and Shim 2016). In this article, we find that appears MCF-7/ADR cells have more significant characteristics of EMT than DOX sensitive MCF-7 cells, manifested as the down-regulated of E-cadherin protein and the

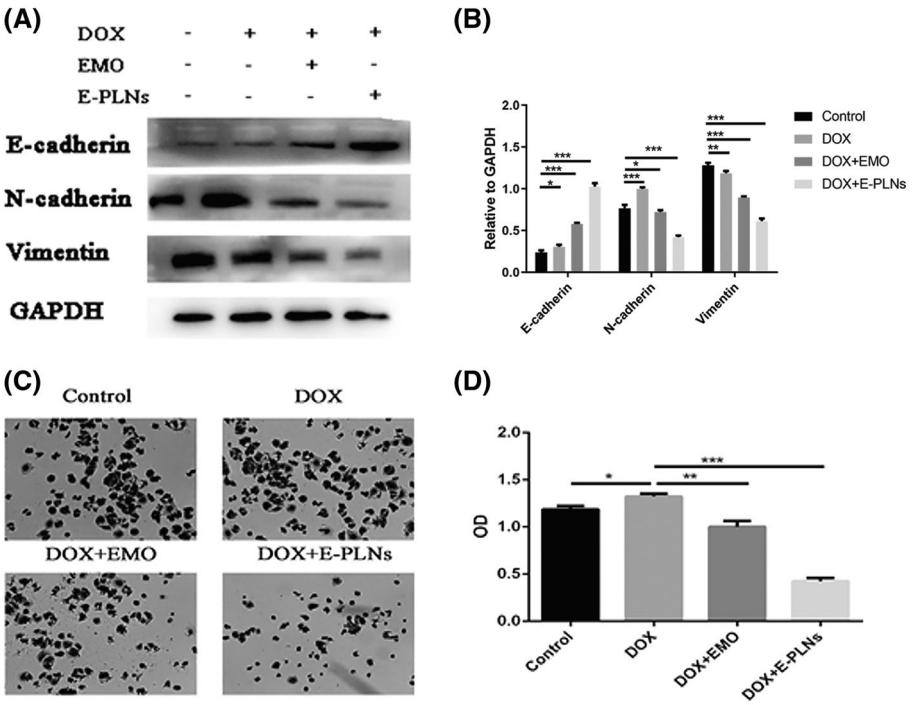

Fig. 8 E-PLNs combined with DOX inhibited EMT marker protein expression and cell invasion. **A**, **B** After MCF-7/ADR cells treated with DOX, DOX + EMO, DOX + E-PLNs for 48 h, the expression of E-cadherin, N-cadherin and Vimentin were detected by Western blotting analysis. **C**, **D** The invasion activity of MCF-7/ADR cells after incubation with DOX, DOX + EMO, DOX + E-PLNs for 24 h. $N = 3$, $^{**}p < 0.01$, $^{***}p < 0.001$ compared with DOX group

up-regulated of N-cadherin protein and Vimentin. Li and his colleagues also confirmed that DOX could induce EMT and apoptosis in MCF-7 cells (Li et al. 2020). The invasion and metastasis are significantly enhanced in tumor cells with EMT characteristics. Indeed, the invasion test showed that MCF-7/ADR cells had more invasive cells than MCF-7 cells, which proved that MCF-7/ADR cells had stronger invasion ability.

Transforming growth factor beta (TGF-β) signaling plays a key role in epithelial-mesenchymal transition (EMT) of tumors (Xu et al. 2009). Galunisertib is a selective TGF-β receptor type I (TGF-βRI) kinase inhibitor which blocking TGF-β signaling reverse EMT (Xu et al. Rodón et al. 2015). The direct toxicity of DOX to cells was enhanced by Galunisertib, which decreased cell viability and increase cell invasion. Moreover, the apoptosis induction in MCF-7/ADR cells of DOX restored after EMT suppression. In addition, previous studies have shown that both P-gp and ATP binding cascade transporters are regulated by EMT. In this study, as the number of cells with EMT characteristics were decreased, and the expression of P-gp protein was restrained. Therefore, it is worth to confirm that EMT participates in the drug resistance of cancer cells by regulating the processes of apoptosis and drug resistance proteins expression.

EMO has been found to increase sensitivity of breast cancer to DOX and PTX (Li et al. 2020; Gu et al. 2020), and inhibit EMT in triple negative breast cancer (Song et al. 2018). It is reported that solid lipid nanoparticles of EMO can significantly block the cell cycle and induce apoptosis of MCF-7 cells compared with free EMO (Wang et al. 2012), which

indicates that lipid nanoparticles delivering EMO may be a promising method for cancer treatment. In this research, we prepared PLNs encapsulated EMO to enhance cellular uptake. As E-PLNs have no fluorescence, the C-6 PLNs are formulated to analyze the cellular uptake of PLNs carriers. The result shown that C-6 PLNs can be absorbed by MCF-7/ADR cells, and quantitative analysis of the average fluorescence intensity shown that PLNs improve the uptake of C-6. Furthermore, the cellular uptake and anti-tumor effect of DOX improved with the combination of E-PLNs, indicated that EMO enhanced the therapeutic effect of DOX on tumor cells. The main mechanisms of the anti-cancer effect in DOX are apoptosis induction. The flow cytometry shown that the apoptosis rate in MCF-7/ADR increased to 24.48% combined with the administration of DOX and E-PLNs. The apoptosis is activated by the increase of Bax/Bcl-2 ratio. The expression of P-gp is restrained with the administration of DOX and E-PLN, resulting in the decrease of DOX efflux. The up-regulated expression of E-cadherin, and down-regulated N-cadherin and Vimentin in MCF-7/ADR cells incubated with E-PLNs indicate that E-PLNs inhibit EMT, therefore reverse DOX resistance in MCF-7/ADR cells.

In this study, we find that EMT is involved in drug resistance, which is related to the regulation of apoptosis and the expression of drug resistance transporters. EMT is one of the key factors to induce DOX resistance in breast cancer. We also found that the expression of E-cadherin in DOX + E-PLNs group was higher than that in DOX group, while the expression of Vimentin and N-cadherin was down-regulated. In addition, when E-PLNs were combined with DOX, the number of invasive cells decreased significantly. These results suggested that E-PLNs enhancing the sensitivity of breast cancer to DOX depended on inhibiting EMT, see Fig. 9.

Conclusion

Drug resistance in tumor is a phenomenon which the continuous administration of chemotherapeutic drugs induces drug tolerance. EMT is one of the possible ways causing DOX resistance in breast cancer. Our data suggested that the DOX resistance in breast cancer is associated with EMT. E-PLNs enhance the sensitivity of DOX in breast cancer via the suppression of EMT. We confirmed that E-PLNs enhance the effect of DOX, which is closely related to the regulation of EMT thereby inhibiting of apoptosis resistance and P-gp expression. The combination of E-PLNs and DOX provides a new scheme for clinical treatment. It is potential that E-PLNs turn into an adjuvant therapy drugs of breast cancer in the feature. Further investigations in animal models and mechanism are warranted.

Materials and methods

Materials

Emodin (> 98% purity) were provided by institute for drug control (Guangzhou, China). Mannitol was purchased from Aladdin Biotech Co., Ltd. (Shanghai, China). Doxorubicin hydrochloride was obtained from Selleck Chemicals (TX, USA). Galunisertib (LY2157299) was obtained from Beyotime Biotechnology (Shanghai, China). P-glycoprotein primary antibodies and was purchased from Abcam (Cambridge, UK). Annexin V-APC dye was provided by KeyGEN BioTECH (Jiangsu, China). Propidium iodide (PI) staining buffer was obtained from BD Biosciences Pharmingen (Shanghai,

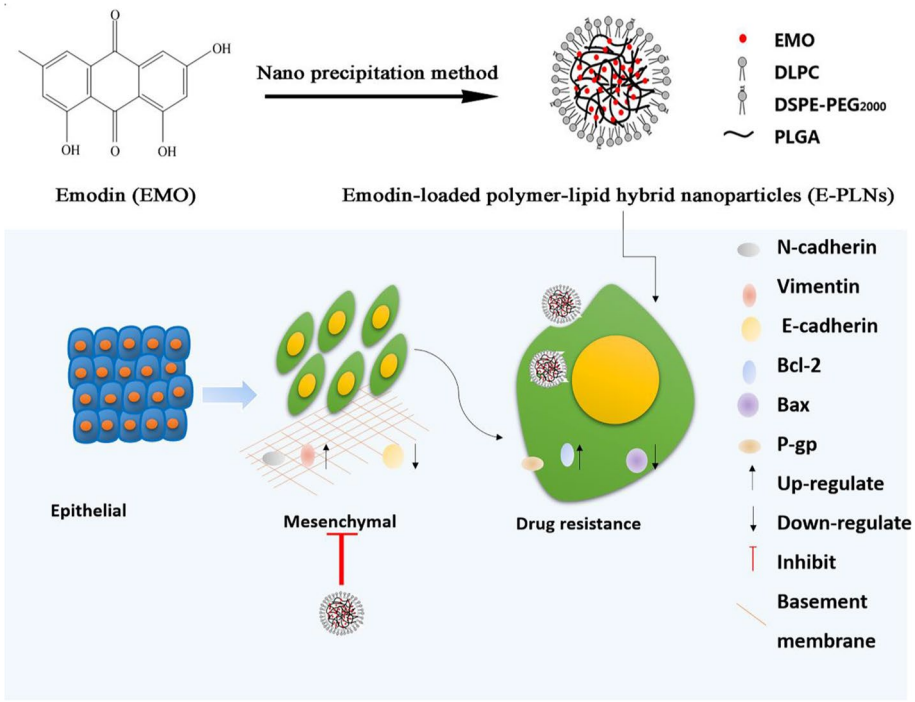

Fig. 9 E-PLNs enhance the sensitivity of breast cancer to doxorubicin by inhibiting epithelial–mesenchymal transition

China). E-cadherin, N-cadherin and Vimentin primary antibodies were purchased from CST, Inc (Massachusetts, USA). Human breast MCF-7 cells and MCF-7/ADR human breast cancer DOX resistant cells were purchased from KeyGen BioTECH (Jiangsu, China).

Preparation of E-PLNs lyophilized powder

We prepared E-PLNs by nano precipitation method (Tahir et al. 2019). Briefly, EMO and PLGA were dissolved in acetone. Another soybean phospholipid and DEPE-PEG 2000 were dissolved in 5% (W/V) F68 aqueous solution. The organic phase was slowly and evenly added to Pluronic F-68 aqueous solution at 75 ℃, and stirred (8000 rpm for 40 min) until the acetone completely evaporated. The supernatant was collected by centrifugation (1000 rpm for 5 min). The particle size and Zeta potential of E-PLNs were measured by Malvern Zetasizer Nano ZS90. The prepared E-PLNs were added with 10% (W/V) freeze-drying protective agent (Mannitol). After being frozen overnight at − 80 ℃, E-PLNs were freeze-dried for 24 h and stored at 4 ℃.

Cell culture

MCF-7 cells were cultured in 10% FBS of RPMI-1640 medium under defined circumstances. To maintain cell resistance to DOX, MCF-7/ADR cells were cultured in RPMI-1640 medium containing DOX (250 ng/mL) every third passage.

Cellular uptake

Coumarin-6 (200 μg/mL) was encapsulated in PLNs instead of EMO to prepare coumarin-6 PLNs (C-6 PLNs). MCF/ADR were incubated with C-6 PLNs for 2 h, fixed by 4% paraformaldehyde, and treated with Hochest staining solution for 5 min. The uptake of C-6 PLNs in MCF/ADR was observed under laser confocal microscope and analyzed by flow cytometry.

Cell viability and resistance index assay

Cells were cultured in 96 well plate for 24 h. Then the fresh culture medium containing free DOX, free EMO, E-PLNs, DOX + EMO, DOX + E-PLNs were added to the culture medium, and cultured for more than 48 h for cell test. After incubation with MTT (5 mg/mL, 20 μL/well) for 4 h, the supernatant was removed. The cells were exposed to DMSO solution (150 μL/well) and incubated for 15 min. Finally, the OD value was detected (Microplate Reader, 490 nm) and cell viability was calculated.

The resistance index (RI) was defined as the ratio of the IC50 of the drug resistant cell line (MCF-7/ADR cells)/IC50 of MCF-7 cells (Sun et al. 2020). Chemo-resistant cancer cell line was determined when RI of cancer cells showed 3 or more.

Cell invasion assay

Cells were resuspended in RPMI-1640 medium without FBS, then seed in the upper chamber for 24 h, and 500 μL culture medium containing different drugs was added into the lower chamber. Cells were fixed with 4% paraformaldehyde for 10 min and stained with 200 μL crystal violet staining solution for 15 min. 5 fields of vision were randomly selected under a 100 × microscope to observed the cells passing through the filter membrane. After taking photos, 500 μL 33% acetic acid solution was added, shaking for 10 min, the OD value was measured to indirectly reflect the number of invasive cells.

Apoptosis study

MCF-7/ADR cells (3 × 105 cells/well, 6 well plate) were cultured, then treated with fresh medium containing different drugs for 48 h. The cells were digested with trypsin without EDTA. After centrifugation again, cells were suspend with 500 μL binding buffer. Then, Annexin-V/FITC and PI staining solution was added with 5 μL each and mixed thoroughly. All experimental groups were sincubated in the dark for 15 min. Finally, the apoptosis was detected on the flow cytometer.

Western blotting analysis

Treated with different treatments for 48 h, cells were lysed with lysate, and the protein was obtained by centrifugation (10,000 rpm for 5 min). BCA method was used to determine the protein concentration. After the expressed proteins (30 μg each) were separated by SDS-PAGE (Bio RAD), and transferred to PVDF membrane. The unbound protein sites were blocked with 5% skim milk for 2 h. The PVDF membrane was incubated with solution containing with different primary antibodies at 4 ℃ overnight. After washed with PBST for 1 h, The PVDF membrane incubated with solution containing

horseradish peroxidase bound secondary antibody for 2 h. The PVDF membrane was evenly coated with ECL developer. According to the manual, the exposure was carried out with chemiluminescence imaging system and analyzed with Image J software.

Statistical analysis

The experiment was repeated three times, and the average value ± SD value was calculated. GraphPad Prism software analyzes and draws pictures, and the one-way anova analysis is used for significance. $^{*}p < 0.05$, $^{**}p < 0.01$, and $^{***}p < 0.001$ are considered to be significantly different.

Abbreviations

EMT: Epithelial–mesenchymal transition; EMO: Emodin; E-PLNs: Emodin-loaded polymer-lipid hybrid nanoparticles; DOX: Doxorubicin; TGF-β: Transforming growth factor beta; TME: Tumor microenvironment; P-gp: P-glycoprotein; PDI: Polydispersity index; Bcl-2: B-cell lymphoma 2; Bax: Bcl-2-associated X protein; GAPDH: Glyceraldehyde 3-phosphate dehydrogenase; PI: Propidium iodide; DAPI: 4′,6-Diamidino-2-phenylindole; PLGA: Poly (lactic-*co*-glycolic acid).

Acknowledgements

Not Applicable.

Authors' contributions

TZ designed the experimental protocols, performed the experiments and analyzed the results. ML, LL, TC and YC contributed to writing the manuscript. FL and HT revised the manuscript. All authors reviewed the final draft of the manuscript. All authors read and approved the final manuscript.

Funding

This work was supported by the Natural Science Foundation of Guangdong (2021A1515011241) and Foshan 'Summit Plan' of building high-level hospitals.

Availability of data and materials

The data will be available if needed.

Declarations

Ethics approval and consent to participate

Not applicable.

Consent for publication

All authors agree with the publication of this manuscript in this journal.

Competing interests

The authors declare that there is no conflict of interest.

Author details

[1]College of Pharmacy, Jinan University, Guangzhou 510632, People's Republic of China. [2]College of Life Sciences, Liaoning University, Shenyang 110036, People's Republic of China. [3]Foshan Hospital of Traditional Chinese Medicine, Foshan 528000, People's Republic of China. [4]Guangdong Key Lab of Traditional Chinese Medicine Information Technology, Jinan University, Guangzhou 510632, People's Republic of China.

Received: 29 April 2021 Accepted: 28 July 2021
Published online: 11 August 2021

References

Asiedu MK, Beauchamp-Perez FD, Ingle JN, Behrens MD, Radisky DC, Knutson KL (2014) AXL induces epithelial-to-mesenchymal transition and regulates the function of breast cancer stem cells. Oncogene 33:1316–1324

Date AA, Joshi MD, Patravale VB (2007) Parasitic diseases: liposomes and polymeric nanoparticles versus lipid nanoparticles. Adv Drug Deliv Rev 59(6):505–521

Du B, Shim JS (2016) Targeting epithelial–mesenchymal transition (EMT) to overcome drug resistance in cancer. Molecules 21:965

Fu JM, Zhou J, Shi J, Xie JS, Huang L, Yip AY, Loo WT, Chow LW, Ng EL (2012) Emodin affects ERCC1 expression in breast cancer cells. J Transl Med 10(Suppl 1):S7

Gu J, Cui CF, Yang L, Wang L, Jiang XH (2019) Emodin inhibits colon cancer cell invasion and migration by suppressing epithelial–mesenchymal transition via the Wnt/β-Catenin pathway. Oncol Res 27:193–202

Gu M, Zheng W, Zhang M, Dong X, Zhao Y, Wang S, Jiang H, Zheng X (2020) LncRNA NONHSAT141924 promotes paclitaxel chemotherapy resistance through p-CREB/Bcl-2 apoptosis signaling pathway in breast cancer. J Cancer 11:3645–3654
Iyer VV, Priya PY, Kangeyavelu J (2018) Effects of increased accumulation of doxorubicin due to emodin on efflux transporter and LRP1 expression in lung adenocarcinoma and colorectal carcinoma cells. Mol Cell Biochem 449(1–2):91–104
Jain V, Kumar H, Anod HV, Chand P, Gupta NV, Dey S, Kesharwani SS (2020) A review of nanotechnology-based approaches for breast cancer and triple-negative breast cancer. J Control Release 326:628–647
Jiang ZS, Sun YZ, Wang SM, Ruan JS (2017) Epithelial–mesenchymal transition: potential regulator of ABC transporters in tumor progression. J Cancer 8:2319–2327
Kalyane D, Raval N, Maheshwari R, Tambe V, Kalia K, Tekade RK (2019) Employment of enhanced permeability and retention effect (EPR): nanoparticle-based precision tools for targeting of therapeutic and diagnostic agent in cancer. Mater Sci Eng C Mater Biol Appl 98:1252–1276
Li W, Zhang H, Assaraf YG, Zhao K, Xu X, Xie J, Yang DH, Chen ZS (2016) Overcoming ABC transporter-mediated multidrug resistance: molecular mechanisms and novel therapeutic drug strategies. Drug Resist Updat 27:14–29
Li S, Fan Y, Kumagai A, Kawakita E, Kitada M, Kanasaki K, Koya D (2020) Deficiency in dipeptidyl peptidase-4 promotes chemoresistance through the CXCL12/CXCR4/mTOR/TGFβ signaling pathway in breast cancer cells. Int J Mol Sci 21:805
Liu Q, Hodge J, Wang J, Wang Y, Wang L, Singh U, Li Y, Yao Y, Wang D, Ai W, Nagarkatti P, Chen H, Xu P, Murphy EA, Fan D (2020a) Emodin reduces breast cancer lung metastasis by suppressing macrophage-induced breast cancer cell epithelial–mesenchymal transition and cancer stem cell formation. Theranostics 10:8365–8381
Liu Q, Hodge J, Wang J, Wang Y, Wang L, Singh U, Li Y, Yao Y, Wang D, Ai W, Nagarkatti P, Chen H, Xu P, Murphy EA, Fan D (2020b) Emodin reduces breast cancer lung metastasis by suppressing macrophage-induced breast cancer cell epithelial–mesenchymal transition and cancer stem cell formation. Theranostics. 10(18):8365–8381
Liu H, Zhuang Y, Wang P, Zou T, Lan M, Li L, Liu F, Cai T, Cai Y (2021) Polymeric lipid hybrid nanoparticles as a delivery system enhance the antitumor effect of emodin in vitro and in vivo. J Pharm Sci 110:2986
Lu J, Xu Y, Wei X, Zhao Z, Xue J, Liu P (2016) Emodin inhibits the epithelial to mesenchymal transition of epithelial ovarian cancer cells via ILK/GSK-3β/Slug signaling pathway. Biomed Res Int 2016:6253280
Markman JL, Rekechenetskiy A, Holler E, Ljubimova JY (2013) Nanomedicine therapeutic approaches to overcome cancer drug resistance. Adv Drug Deliv Rev 65:1866–1879
Mukerjee A, Ranjan AP, Vishwanatha JK (2012) Combinatorial nanoparticles for cancer diagnosis and therapy. Curr Med Chem 19:3714–3721
Mukherjee A, Waters AK, Kalyan P, Achrol AS, Kesari S, Yenugonda VM (2019) Lipid-polymer hybrid nanoparticles as a next-generation drug delivery platform: state of the art, emerging technologies, and perspectives. Int J Nanomedicine 14:1937–1952
Rodón J, Carducci M, Sepulveda-Sánchez JM, Azaro A, Calvo E, Seoane J, Braña I, Sicart E, Gueorguieva I, Cleverly A, Pillay NS, Desaiah D, Estrem ST, Paz-Ares L, Holdhoff M, Blakeley J, Lahn MM, Baselga J (2015) Pharmacokinetic, pharmacodynamic and biomarker evaluation of transforming growth factor-β receptor I kinase inhibitor, galunisertib, in phase 1 study in patients with advanced cancer. Invest New Drugs 33:357–370
Siegel RL, Miller KD, Fuchs HE et al (2021) Cancer statistics, 2021. CA Cancer J Clin 71(1):7–33
Song X, Zhou X, Qin Y, Yang J, Wang Y, Sun Z, Yu K, Zhang S, Liu S (2018) Emodin inhibits epithelial–mesenchymal transition and metastasis of triple negative breast cancer via antagonism of CC-chemokine ligand 5 secreted from adipocytes. Int J Mol Med 42:579–588
Sun Y, Wang X, Zhou Q, Lu Y, Zhang H, Chen Q, Zhao M, Su S (2015) Inhibitory effect of emodin on migration, invasion and metastasis of human breast cancer MDA-MB-231 cells in vitro and in vivo. Oncol Rep 33:338–346
Sun M, He L, Fan Z, Tang R, Du J (2020) Effective treatment of drug-resistant lung cancer via a nanogel capable of reactivating cisplatin and enhancing early apoptosis. Biomaterials 257:120252
Sung H, Ferlay J, Siegel RL et al (2021) Global cancer statistics 2020: GLOBOCAN estimates of incidence and mortality worldwide for 36 cancers in 185 countries. CA Cancer J Clin 71:209
Tahir N, Madni A, Correia A, Rehman M, Balasubramanian V, Khan MM, Santos HA (2019) Lipid-polymer hybrid nanoparticles for controlled delivery of hydrophilic and lipophilic doxorubicin for breast cancer therapy. Int J Nanomedicine 14:4961–4974
Wang S, Chen T, Chen R, Hu Y, Chen M, Wang Y (2012) Emodin loaded solid lipid nanoparticles: preparation, characterization and antitumor activity studies. Int J Pharm 430:238–246
Xu J, Lamouille S, Derynck R (2009) TGF-beta-induced epithelial to mesenchymal transition. Cell Res 19:156–172

Publisher's Note